Plasma synthesis of ammonia in a tangled wire dielectric barrier discharge reactor: Effect of electrode materials

Yichen Ma, Yuxing Tian, Yuxuan Zeng, Xin Tu

PII: S1743-9671(21)00157-4

DOI: https://doi.org/10.1016/j.joei.2021.09.002

Reference: JOEI 957

To appear in: *Journal of the Energy Institute*

Received Date: 12 July 2021

Revised Date: 29 August 2021

Accepted Date: 2 September 2021

Please cite this article as: Y. Ma, Y. Tian, Y. Zeng, X. Tu, Plasma synthesis of ammonia in a tangled wire dielectric barrier discharge reactor: Effect of electrode materials, *Journal of the Energy Institute* (2021), doi: https://doi.org/10.1016/j.joei.2021.09.002.

Plasma synthesis of ammonia in a tangled wire dielectric barrier discharge reactor: Effect of electrode materials

Yichen Ma, Yuxing Tian, Yuxuan Zeng, Xin Tu*

Department of Electrical Engineering and Electronics, University of Liverpool, Liverpool, L69 3GJ, UK

***Corresponding Author**

Prof. Xin Tu
Department of Electrical Engineering and Electronics,
University of Liverpool,
Liverpool, L69 3GJ,
UK
E-mail: xin.tu@liverpool.ac.uk

Abstract

Plasma synthesis of NH_3 from N_2 and renewable H_2 under mild conditions is very attractive for decentralised sustainable green ammonia production using intermittent renewables. In this study, NH_3 synthesis was performed under ambient conditions in a dielectric barrier discharge (DBD) plasma reactor. Different tangled wire internal electrodes were employed to understand the influence of electrode materials on plasma ammonia synthesis. Compared with a rod electrode, a tangled wire electrode substantially enhanced the NH_3 concentration and reduced the energy cost for ammonia production, which can be attributed to the expanded surface area and the chemisorption properties of the tangled electrodes. The influence of the N_2/H_2 molar ratio and total flow rate on the reaction performance was also evaluated. The lowest energy cost (59.0 MJ $mol_{NH_3}^{-1}$) for ammonia production was achieved using a Cu tangled electrode at a total flow rate of 250 ml min^{-1} and a discharge power of 20 W. The electrical diagnostics of the plasma process showed that the tangled wire electrodes decreased the breakdown voltage of the DBD and enhanced charge deposition, which enhanced the NH_3 production. The reaction mechanism was discussed for the process optimisation of ammonia synthesis in a tangled wire DBD system.

Keywords: Ammonia synthesis; Dielectric barrier discharge; Non-thermal plasma; Electrode materials; Nitrogen fixation

1. Introduction

Recent years have witnessed a rising demand for ammonia due to its vital role in the chemical and agricultural sectors. The estimated global production of ammonia is over 160 million tonnes each year, and approximately 80% of the ammonia is consumed in fertiliser production [1]. The advent of synthetic nitrogen fertiliser has led to fundamental changes in food production and now feeds nearly half of the world's population [2]. Nowadays, ammonia is being considered as a carbon-free energy storage vector for the long-distance transport of hydrogen due to its large hydrogen mass density and the mild temperature required for liquefaction [3]. It is also promising for short-term electrochemical energy storage (i.e. batteries) to deliver on-demand energy in conjunction with fuel cells, which would enable better uptake of the irregular supply from sustainable electricity [4]. Nevertheless, conventional ammonia synthesis via the Haber-Bosch (H-B) process takes up 1-2% of the global energy consumption and releases more than 300 tonnes of CO_2 on an annual basis [5, 6]. Success in developing green, efficient, and commercially viable alternatives to the H-B process that accommodate renewable energy and CO_2-free hydrogen will reinforce the importance of ammonia in traditional fertiliser production and pioneering energy storage.

Although the ammonia synthesis from N_2 and H_2 is exothermic (R1), elevated temperatures (~700 K) are needed for the dissociation of the robust dinitrogen triple bond, which is the rate-limiting step in the H-B process [7]. In the context of high temperatures, high pressures around 100 bar are required to shift the equilibrium towards the formation of ammonia. The harsh conditions of the H-B process require large-scale centralised plants and continuous operation with an uninterrupted power supply. Thus, activating the inert dinitrogen at lower temperatures and lower pressures would be significant for addressing these challenges and improving the processes efficiency [8].

$$N_2 + 3H_2 \rightleftharpoons 2NH_3 \qquad \Delta H_{298K} = -46.27\ \mathrm{kJ/mol} \qquad \text{(R1)}$$

Non-thermal plasma (NTP) has been considered as an ideal candidate for sustainable N_2 fixation under mild conditions [9]. In an NTP, highly energetic electrons with a mean electron energy of 1-10 eV are initially generated, inducing a cascade of chemically reactive species (e.g., excited molecules, ions, and atoms) that facilitates the kinetically limited dinitrogen activation at low bulk gas temperatures [10-13]. This unique feature

enables the plasma-driven ammonia synthesis to be performed under thermodynamically favourable conditions at atmospheric pressure. Due to the mild working conditions, the NTP technology is compact, flexible, and easily switched on and off; this is desirable for the accommodation of intermittent and highly decentralised renewable energy sources such as solar, wind, and tidal energy for the decentralised small-scale green ammonia production [14, 15]. Moreover, the NTP process can readily integrate with water electrolysis using intermittent renewable electricity to achieve net-zero ammonia synthesis and alleviate the environmental impact [16].

In recent years, considerable efforts have been devoted to the plasma synthesis of ammonia using dielectric barrier discharges (DBDs) [17-23]. Bai et al. reported plasma synthesis of NH_3 in a cylindrical DBD reactor at ambient conditions [20]. Wang et al. developed a unique water-cooled DBD reactor for the synthesis of ammonia at near room temperature and ambient pressure [21]. Aihara et al. employed a metallic wire electrode to synthesise ammonia in a DBD reactor, achieving an NH_3 yield of 3.5% and an energy cost of 18.6 MJ $mol_{NH_3}^{-1}$. Their results proved that using a metal wire as the high-voltage inner electrode contributes to a more productive ammonia synthesis via the increased surface area [22]. Besides, Iwamoto et al. [23] and Mehta et al. [24] evaluated the activities of different metals via density functional theory (DFT) calculations and microkinetic modelling. The employment of proper metal electrodes in a DBD reactor can open a new route to tailor the formation of reactive species and facilitate ammonia production. However, reducing the energy cost and enhancing the ammonia yield remain challenges that require further innovation and improvement in plasma reactor design. Moreover, the individual effect of metallic electrodes such as electrode materials and electrode configurations on the electrical properties of the discharge is still underexplored in plasma NH_3 synthesis [25, 26]. Further efforts are required to develop a systematic understanding of these fundamental plasma properties in ammonia synthesis, this will reduce the energy consumption of NH_3 production under ambient conditions, shedding light on the reaction mechanism of the plasma ammonia synthesis, and generating essential and invaluable knowledge for the future development of this disruptive and emerging technology.

In this work, the ammonia synthesis from nitrogen and hydrogen was carried out using a DBD reactor with tangled metal electrodes. The influence of process parameters

including the N_2/H_2 molar ratio and total gas flow rate on the NH_3 concentration and energy cost were investigated. The chemical performances and discharge characteristics were also examined using different tangled electrode materials. A possible reaction mechanism was discussed based on the comprehensive analysis of experimental findings with a view to achieving process optimisation of ammonia synthesis in a tangled wire DBD reactor.

2. Experimental

2.1 Experimental setup

In this work, a coaxial DBD reactor was used to investigate the plasma-synthesis of ammonia under ambient conditions. Figure 1(a) shows a schematic diagram of the experimental setup. N_2 and H_2 were controlled by mass flow controllers (Omega, FMA-2404) before being introduced into the DBD reactor. The configuration of the tangled wire DBD reactor is depicted in Figure 1(b). A quartz tube with an outer diameter of 22 mm and a wall thickness of 1.5 mm was used as the dielectric layer. A stainless-steel mesh wrapped around the quartz tube served as a ground electrode, while a metal rod or a loose metal-wool was placed in the middle of the quartz tube and acted as the high voltage electrode. Several metals were used as the tangled wire electrodes, including NiFe alloy, stainless steel (SS), Ti, and Cu. These wires were comprised of fibres with the same diameter (0.2 mm) and total length (10 m), thus providing the same surface area (63 cm^2). The discharge length was 80 mm with an average effective discharge gap of 8 mm. A hollow stainless-steel rod electrode with an outer diameter of 14 mm was used for comparison, as shown in Figure 1(c). The DBD reactor was connected to a high voltage AC power supply with a maximum peak voltage of 30 kV and a frequency of 5-20 kHz. The voltage on an external capacitor (C_{ext} = 0.47 μF) connected to the ground electrode was measured to determine the total charge (Q_{ext}) transferred in the plasma, while the applied voltage was recorded by a high voltage probe (Testec, TT-HVP 15 HF) and the current was measured by a current monitor (Magnelab, CT-E0.5). All signals were sampled by a 4-channel digital oscilloscope (Tektronix, DPO2024B). A homemade power measurement system was used to monitor and control the discharge power in real-time via the area calculation of the Q-U Lissajous figure. In this work, the discharge power was fixed at 20 W.

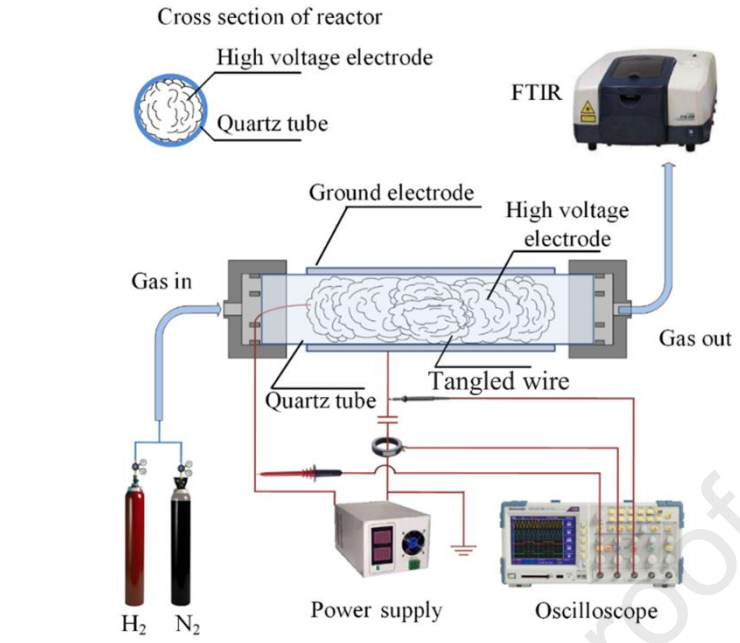

(a)

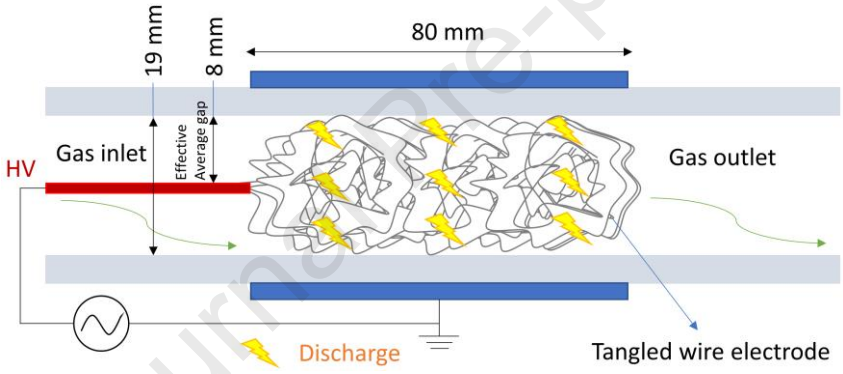

(b)

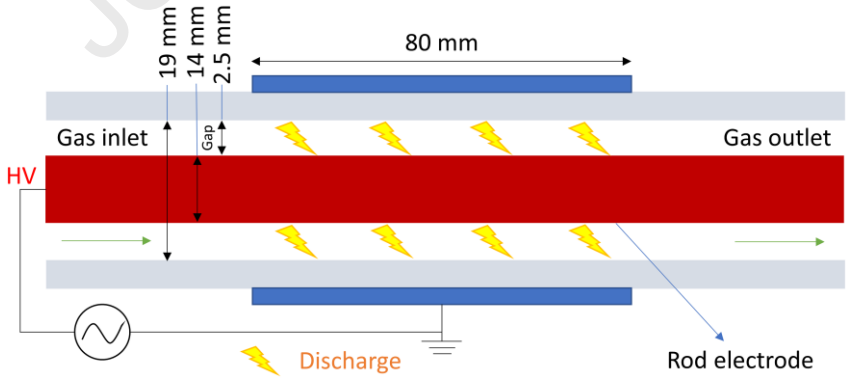

(c)

Figure 1. (a) Schematic diagram of the experimental setup; (b) configuration of the tangled wire DBD reactor; (c) configuration of the rod electrode DBD reactor.

2.2 Product analysis

A gas mixture with a variable N_2/H_2 molar ratio was used as the reactants and the total feed flow rate was controlled between 50 and 250 ml min^{-1} during the experiment. The reaction products were analysed by a Fourier transform infrared (FTIR) spectrometer (Jasco, FTIR-4200) with a resolution of 2 cm^{-1}. It contained a gas cell with an optical pathlength of 10 cm (Specac, Storm 10 gas cell). The concentration of ammonia in the product gas was calculated using a series of calibration gas mixtures. The gas products were sampled every five minutes to monitor the time-resolved performances of this DBD system, while the NH_3 concentration was recorded after 120 min running time for each test. Each measurement was repeated three times, and the margin of error in this work was within 3%.

In the ammonia synthesis process, the conversion of N_2 and H_2 is defined as:

$$X_{N_2} = \frac{\text{moles of } N_2 \text{ converted}}{\text{moles of } N_2 \text{ input}} \times 100 \quad (1)$$

$$X_{H_2} = \frac{\text{moles of } H_2 \text{ converted}}{\text{moles of } H_2 \text{ input}} \times 100 \quad (2)$$

The energy cost (*EC*) of ammonia synthesis is defined as:

$$EC \text{ (MJ mol}_{NH_3}^{-1}) = \frac{\text{discharge power (W)}}{\text{moles of } NH_3 \text{ per second (mol/s)}} \times \frac{1}{10^6 \left[\frac{\text{J}}{\text{MJ}}\right]} \quad (3)$$

2.3 Evaluation of electrical parameters

Figure 2(a) illustrates the classic equivalent circuit of a DBD reactor, in which C_{diel} and C_{gap} correspond to the capacitance of the dielectric layer and the capacitance of the discharge gap, respectively. In the presence of a packing material, C_{gap} includes the contribution of the gas-solid integration in between the electrodes. Conductive filaments are formed when the gas breakdown happens, thus the switch 'K' in the parallel resistive channel is on.

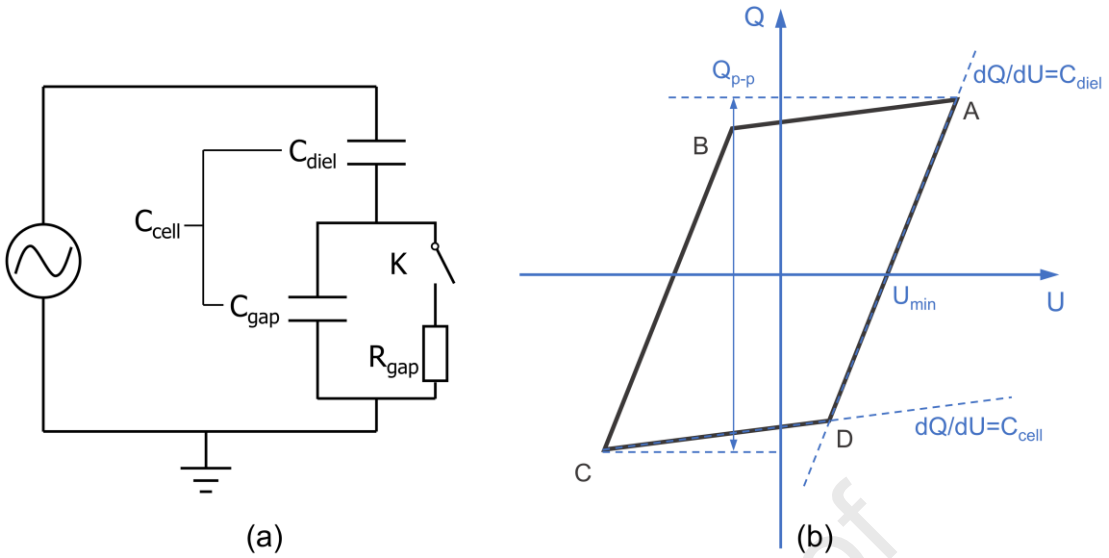

Figure 2. (a) The equivalent electrical circuit of a DBD reactor and (b) a typical Q-U Lissajous plot of the DBD.

The shape of a Q-U Lissajous figure typically approximates a parallelogram where the internal electrical discharge characteristics can be derived from its dimensions, including the breakdown voltage, reactor charge, and reactor capacitance [27]. Figure 2(b) demonstrates a typical Q-U Lissajous figure from which the charges transferred per half-cycle (Q_{trans}) can be obtained. The lines AB and CD in a Lissajous figure stand for the plasma-off period. The slope dQ/dU of these lines equals C_{cell} in this period, which comprises the gap capacitance C_{gap} and the dielectric capacitance C_{diel}:

$$\frac{1}{C_{cell}} = \frac{1}{C_{diel}} + \frac{1}{C_{gap}} \tag{4}$$

Therefore, the gap capacitance C_{gap} can be expressed as follows:

$$C_{gap} = \frac{C_{diel} \times C_{cell}}{C_{diel} - C_{cell}} \tag{5}$$

The lines BC and DA in the Lissajous plot correspond to the plasma-on phase. The slope of these lines corresponds to the effective capacitance C_{eff} which equals the dielectric capacitance C_{diel} in a fully bridged gap [28].

The total charge in the plasma Q can be calculated from the voltage U_c on an external capacitor C_{ext} (0.47 μF), and the voltage on the dielectric material U_d can be calculated using charge Q and C_{diel}:

$$Q = C_{ext} \times U_c \tag{6}$$

$$U_d = \frac{Q}{C_{diel}} \quad (7)$$

Accordingly, the gas voltage U_g across the discharge gap is obtained from the applied voltage U_a and dielectric voltage U_d:

$$U_g = U_a - U_d \quad (8)$$

The breakdown voltage U_b can be calculated using U_{min} from the Lissajous figure as follows [29, 30]:

$$U_b = \frac{1}{1 + C_{gas} / C_{diel}} \times U_{min} \quad (9)$$

3. Results and discussion

3.1 Effect of electrode materials on the plasma-driven NH_3 synthesis

Figure 3 shows the influence of different electrode materials on ammonia synthesis in terms of NH_3 concentration and energy cost for ammonia production. Compared with the rod electrode, the NH_3 production was more efficient using the tangled wire electrodes, this can be attributed to the larger surface area (63 cm^2) of the tangled wire electrode compared to the rod electrode (45 cm^2). Besides, it was reported that the surface of the tangled wire electrode became bumpy after the plasma treatment, which further expands the surface area and facilitates the synthesis of ammonia [22]. Among the tangled electrodes, copper had the most optimal synthesis performance with an N_2 conversion of 0.31%, an NH_3 concentration of 2983 ppm, and an energy cost of 90.2 MJ $mol_{NH_3}^{-1}$. The performance of the tangled wire electrodes for the NH_3 synthesis followed the order of Cu > Ti > SS > NiFe, suggesting the plasma-driven ammonia production is affected by the material of the electrodes. Interestingly, in a study of NH_3 decomposition using supported metal catalysts, the activity of the catalysts followed the order of Co > Ni > Fe > Cu, which is the reverse of our NH_3 synthesis study [31]. This finding implies that the favourable performance of copper in this work may be associated with the reduced reverse reaction - decomposition of formed NH_3 on the electrode surface.

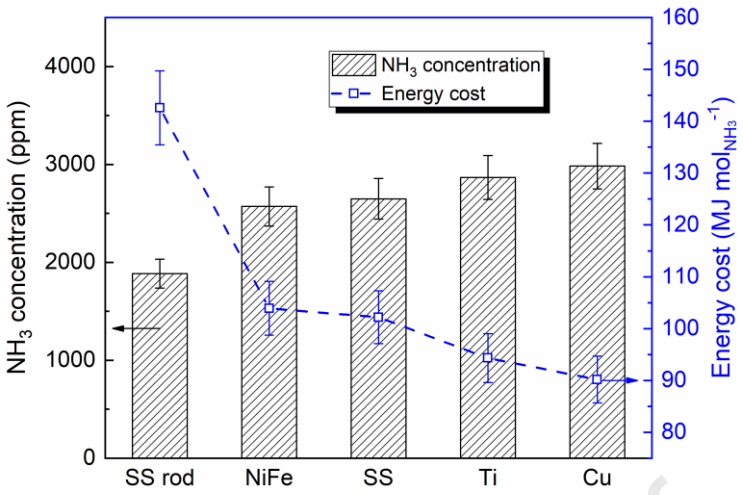

Figure 3. Effect of different electrode materials on NH_3 production and the energy cost. (N_2/H_2 = 1:1, total flow rate 100 ml min^{-1}, discharge power 20 W)

Table 1. The N_2 and H_2 conversion in the NH_3 synthesis process. (N_2/H_2 = 1:1, total flow rate 100 ml min^{-1} and discharge power 20 W)

Electrode materials	Conversion (%)	
	N_2	H_2
SS Rod	0.19	0.57
NiFe	0.27	0.80
SS	0.27	0.82
Ti	0.30	0.89
Cu	0.31	0.93

3.2 Effect of process parameters on the plasma synthesis of ammonia

Figure 4 shows the effect of the N_2/H_2 molar ratio on the plasma NH_3 synthesis. The NH_3 concentration increased with the elevated N_2 content and reached a maximum at an N_2/H_2 ratio of 1:1, then dropped when further increasing the N_2/H_2 ratio to 3:1. The influence of the N_2/H_2 ratio on the energy cost of NH_3 production showed the reverse trend. As shown in Figure 4, The highest ammonia concentration and the lowest energy cost were achieved at the optimum N_2/H_2 ratio of 1:1. This result is consistent with the findings in previous studies that non-stoichiometric ratios of N_2/H_2 lead to higher ammonia yields than the stoichiometric ratio (1:3) [32-37]. Peng and co-workers reported that the minimum energy cost of plasma-synthesis of NH_3 was achieved at an N_2/H_2 ratio of 1:1 regardless of the applied voltage, and further increasing N_2 content increased the

energy cost [32]. Gomez et al. achieved the lowest energy cost of ammonia production at an N_2/H_2 molar ratio in the range of 1:3 to 1:1 [33]. This phenomenon can be explained by a trade-off between the reaction kinetics of NH_3 synthesis and the discharge properties. Compared with the stoichiometric N_2/H_2 ratio (1:3), higher N_2 concentrations can contribute to a higher fraction of plasma energy deposited in N_2 molecules, facilitating the rate-limiting step of dinitrogen dissociation. However, excessive N_2 content may decrease the mean electron energy in DBD plasmas and suppress the plasma dissociation of N_2 [34].

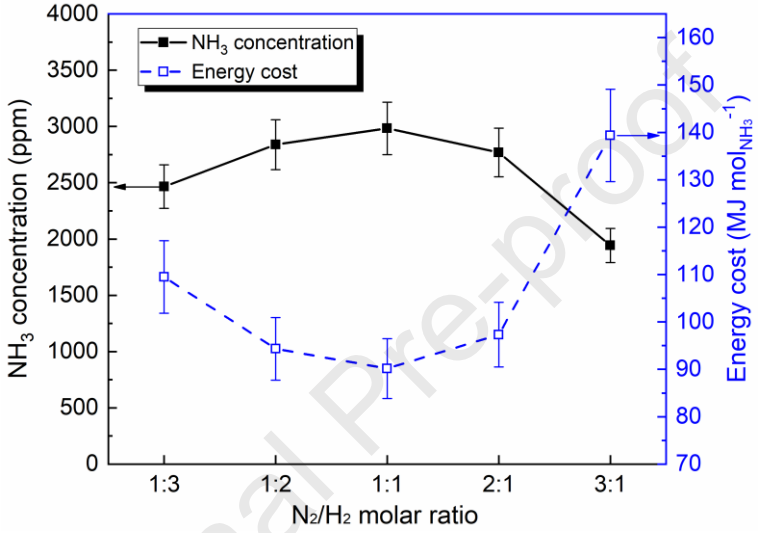

Figure 4. Effect of the N_2/H_2 molar ratio on NH_3 production and the energy cost. (Cu tangled electrode, total flow rate 100 ml min^{-1}, discharge power 20 W)

Figure 5 shows the effect of the total feed flow rate on the NH_3 production and energy cost using the tangled Cu electrode at a constant N_2/H_2 molar ratio of 1:1 and a discharge power of 20 W. The NH_3 concentration declined with the rising total flow rate, which can be ascribed to the decreased residence time in the discharge area reducing the number of collisions of the reactant molecules with energetic electrons and chemically reactive species [32, 38]. Nevertheless, the higher flow rate increases the total number of reactants passing through the plasma zone and enhances the number of converted molecules at a constant discharge power. As a result, the energy cost of ammonia production decreased from 139.3 to 59.0 MJ $mol_{NH_3}^{-1}$ when increasing the total flow rate from 50 to 250 ml min^{-1}.

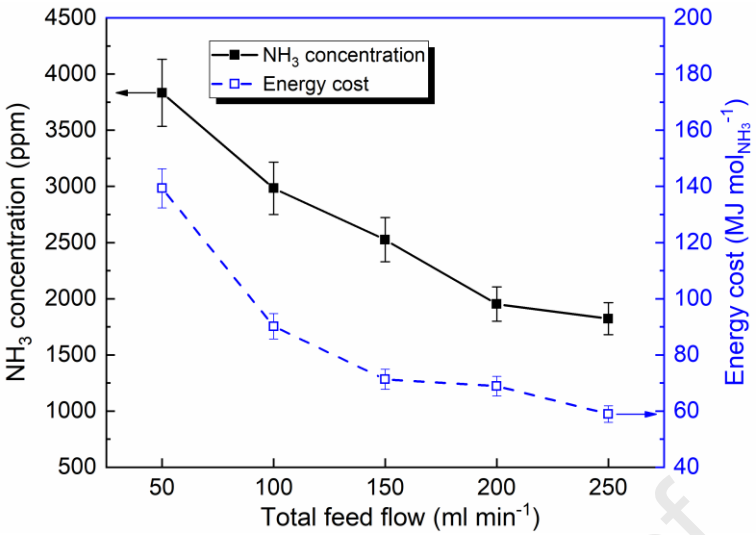

Figure 5. Effect of total flow rate on NH_3 production and energy cost. (Cu tangled electrode, N_2/H_2 molar ratio 1:1, discharge power 20 W)

3.3 Effect on electrical properties when using different electrode materials

Figure 6 shows the time-resolved electrical signals of DBD plasma in the NH_3 synthesis process. The current signals are similar when using different tangled electrode materials, suggesting the discharge model is not changed by varying the electrode. The strong current pulses corresponded to the filamentary discharges bridging the gas gap. As the tangled wire loosely filled the whole discharge gap and was in contact with the inner surface of the quartz tube, the presence of numerous weak current pulses can be attributed to the formation of the local filamentary discharges in between the dielectric layer and the metal wire. The DBD with the tangled Cu electrode showed the highest amplitude of the current pulses. As a result, the chance for collisions between electrons and reactants and the average electron density were enhanced due to the higher discharge current and charge transfer (Table 2). This enhancement in current and charge transfer would increase the chance of collisions between electrons and reactants as well as the average electron density, both of which contribute to the enhanced dissociation of nitrogen molecules, the rate-limiting step in the plasma synthesis of ammonia. The gas voltage became quasi-flat over time after the ignition of the plasma, suggesting that the formation of filamentary discharges is not affected by the applied voltage after the electrical gas breakdown [30]. The gas voltage was in the sequence of SS rod > NiFe > SS > Ti > Cu, consistent with the concentration of synthesised ammonia (Figure 3). This finding can be associated with the production of NH_3 in the plasma reactor: as the dielectric strength of NH_3 is lower

than that of N_2 and H_2, the presence of the produced NH_3 in the DBD reactor changes the dielectric properties of the working gas and thus reduces the breakdown voltage of the DBD.

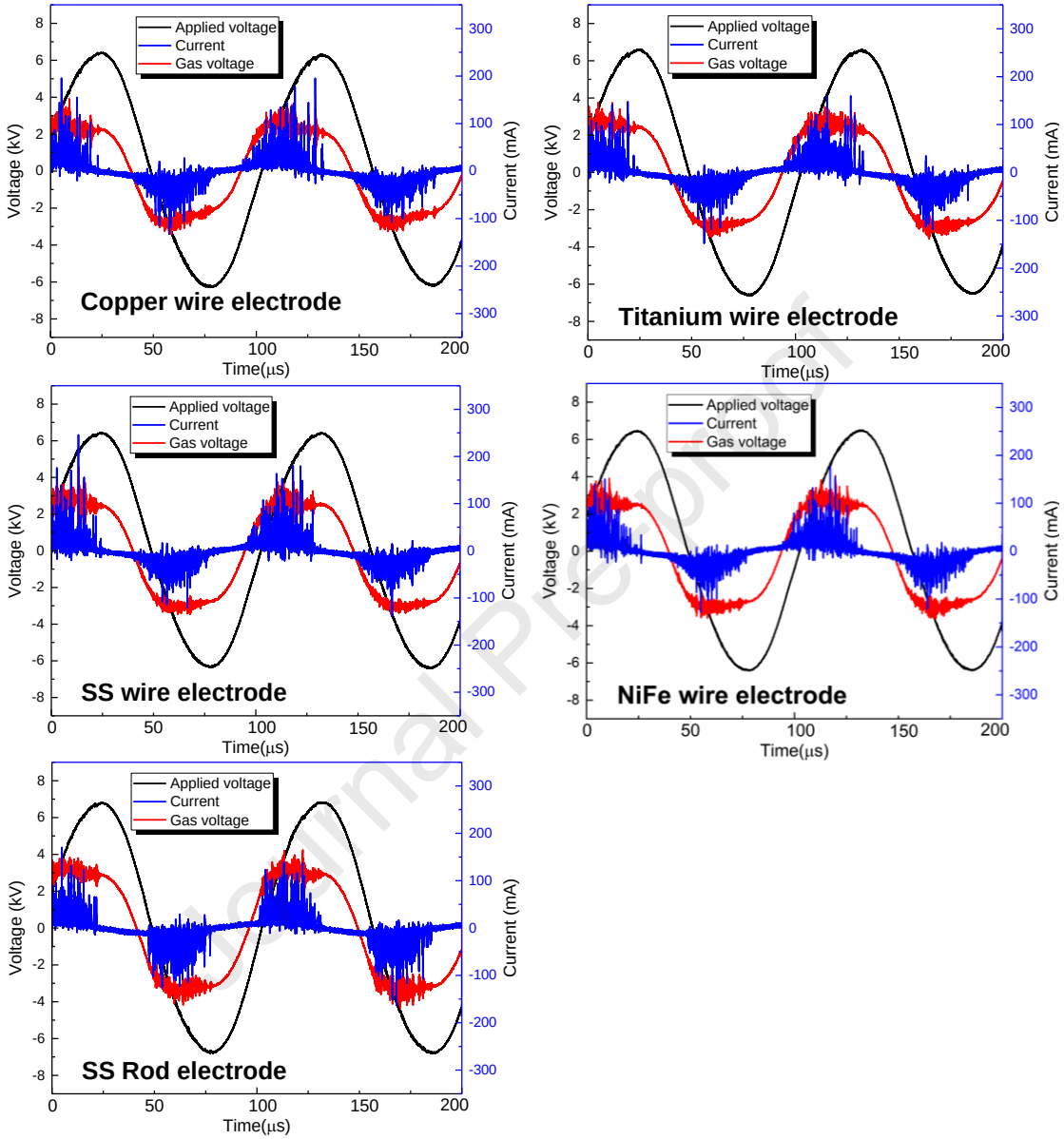

Figure 6. Typical electrical signals of the DBD using different electrodes. (N_2/H_2 = 1:1, total flow rate 100 ml min^{-1}, frequency 9 kHz, discharge power 20 W)

The typical Lissajous plots obtained during the NH_3 synthesis using different inner electrodes are illustrated in Figure 7. The Lissajous figure of the DBD using the SS rod electrode was a strict parallelogram shape, while the Lissajous figure of the discharge morphed to an oval shape when using the tangled electrodes. This also indicates a change in the discharge characteristics. Table 2 summarises the influence of the different electrodes on the peak-to-peak applied voltage (U_{pp}) and charge transferred across the

gap during the discharge (Q_{trans}). The use of tangled wire electrodes has a clear effect on the charge characteristics of the DBD plasma. Compared with other electrode materials, the DBD with the Cu wire showed the lowest applied voltage, as well as an enhanced amplitude of the current pulses (Figure 6) and the charge transfer of the discharge.

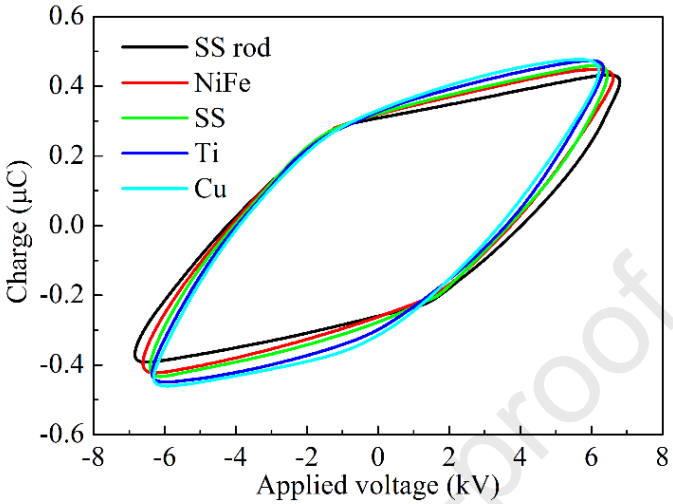

Figure 7. Lissajous figure obtained during the plasma synthesis of NH_3. (N_2/H_2 = 1:1, total flow rate 100 ml min^{-1}, frequency 9 kHz, discharge power 20 W)

Table 2. Electrical properties of the DBD reactor using different electrodes. (N_2/H_2 = 1:1, total flow rate 100 ml min^{-1}, discharge power 20 W)

Electrode material	Q_{trans} (μC)	U_{pp} (kV)
Rod	0.82	13.8
NiFe	0.87	13.3
SS	0.89	13.0
Ti	0.92	12.8
Cu	0.95	12.5

4. Discussion

In the Haber-Bosch process, initially the dissociative adsorption of N_2 and H_2 takes place on the catalyst surface, followed by the step-wise hydrogenation of adsorbed N atoms to form NH_3 (R2-R6, * denotes the adsorption site on the catalyst surface) [39].

$$N_2 + * \longrightarrow 2N(s) \quad \text{(R2)}$$

$$H_2 + * \longrightarrow 2H(s) \quad \text{(R3)}$$

$$N(s) + H(s) \longrightarrow NH(s) \quad \text{(R4)}$$

$$NH(s) + H(s) \longrightarrow NH_2(s) \quad \text{(R5)}$$

$$NH_2(s) + H(s) \longrightarrow NH_3(s) \quad \text{(R6)}$$

In contrast, NTP enables the activation and dissociation of reactants in the gas phase, thus creating new reaction routes for ammonia production. It is well accepted that NTP improves the activity of ammonia synthesis via overcoming the prohibitively high energy barrier for the dissociation of the robust dinitrogen triple bond, generally through four basic channels: direct dissociation, ionisation, electronic excitation, and vibrational excitation [40]. It was reported that the reactions involving radicals and vibrationally-excited molecules are significant in the formation of NH_3 in plasma, while the ions are considered less important [24, 34]. Moreover, the vibrational excitations can facilitate the N_2 dissociation in both gas-phase and surface reactions [19]. The presence of plasma-generated excited intermediates was confirmed using OES diagnostics [41].

The reaction pathways for ammonia synthesis involving surface reactions can be divided into Eley-Rideal (E-R) and Langmuir-Hinshelwood (L-H) reactions [42]. For the E-R mechanism, the H atoms and NH_x intermediates are formed in gas-phase reactions and the ammonia synthesis takes place on the metal surface. More specifically, the NH species generated in the gas phase react with the surface adsorbed H thereby forming ammonia [32, 34]. In the L-H mechanism, the reactive species (e.g., surface-adsorbed N and H atoms) are primarily formed via dissociative adsorption of molecules [43]. Previous experimental and simulation studies proposed the significance of excited molecular N_2 species [23, 24]. Instead of direct dissociation in the gas phase, the N_2 excited states undergo dissociative adsorption to form surface-adsorbed atomic N species. Thereafter, mutual reactions between species adsorbed on the catalyst surface are responsible for ammonia production. In this study, both pathways may take place and contribute to ammonia production.

Iwamoto et al. performed DFT calculations to understand the formation energy (ΔE_f) of metal nitride and the adsorption energy of an N atom on different metal surfaces in a metal-wire DBD reactor [23]. Their studies showed that Cu surfaces are more favourable for adsorption of N atoms compared to Ni, Ti, and Fe surfaces. Shah et al. found the

presence of the intermediate GaN on the surface of a Ga-In alloy catalyst in the plasma-catalytic synthesis of ammonia [44]. Their finding suggests that the formation of the metal nitride on the metal electrode surface also contributes to the ammonia synthesis in a DBD reactor. The high surface area of the metal wire electrodes enables the surface metal sites to derive N atoms from N_2 excited states followed by the subsequent step-wise hydrogenation of N with H to form NH_3.

Table 3 compares the performance of ammonia synthesis using different types of plasma. Note that the energy cost achieved in this work (59.0 MJ $mol_{NH_3}^{-1}$) is strongly competitive compared with other plasma processes. Previous studies also utilised radiofrequency (RF) plasmas and microwave (MW) discharges in NH_3 production; these processes usually achieve high N_2 conversion but consume excessive energy due to high power input [44-46]. Further enhancement of the reaction activity could be achieved by adding suitable catalysts into the plasma, a hybrid plasma-catalytic system has significant potential to take advantage of the low-temperature synergistic effect in ammonia synthesis. Mehta et al. focused on supported metal catalysts and plotted volcano curves of their activity for ammonia synthesis [24]. Compared to conventional heterogeneous catalysis, the optimal catalysts for plasma catalysis are metal sites that weakly bind with nitrogen. Moreover, using different packed-bed materials in a DBD reactor can also affect the formation of a range of reactive species and influence the chemical reactions [33]. For instance, Gómez-Ramírez et al. reported an N_2 conversion of >7% using ceramic-lead zirconate titanate (PZT) pellets in a DBD reactor. Their work showed that the presence of ferroelectric materials enhanced the ammonia production through the influenced discharge properties and the catalytic reactions on the surface of ferroelectric pellets [41]. As innovative plasma reactor design and rational design of catalysts have been considered as feasible strategies to reduce the energy cost of plasma processes, the integration of both strategies could be a promising route for future development.

Table 3. Comparison of key parameters in our study with other plasma processes used for ammonia synthesis.

Plasma	Catalyst	Flow rate (ml min^{-1})	N_2/H_2 ratio	Power (W)	X_{N_2} (%)	*EC* (MJ $mol_{NH_3}^{-1}$)	Ref.
MW	-	15000	9:1	1100	0.75	1532.8	[45]

RF	Ga-In molten alloy	20	1:4	300	-	197.8	[44]
RF	Au wire	20	1:4	300	-	322.7	[46]
RF	Ni-MOF-74	20	1:4	50	-	266.6	[47]
DBD	Ru/Al_2O_3	500	3:2	12	-	95.8	[48]
DBD	Ni/SiO_2	25	1:3	107	6.4	81.7	[49]
DBD	Ni/Al_2O_3	100	1:2	10	-	68.9	[24]
Water-electrode DBD	Ni/Al_2O_3	56	1:2	20	0.09	211.4	[21]
DBD	Ru/alumina membrane	40	1:3	127	4.7	165.7	[50]
DBD	Ru/alumina membrane	30	1:3	127	4.8	153.3	[37]
DBD	Carbon coatings on Al_2O_3	60	1:3	98	2.3	383.2	[19]
DBD	PZT	11.5	1:3	-	7.2	278.7	[41]
DBD	PZT	11.5	1:3	-	2.7	175.2	[33]
DBD	-	250	1:1	20	0.31	59.0	this work

5. Conclusions

The NH_3 synthesis was carried out in a DBD plasma reactor under ambient conditions. A tangled wire electrode was used to improve NH_3 production and decrease energy costs. Compared with the rod electrode, the tangled wire electrode substantially enhanced the conversion of N_2 and H_2, increased the NH_3 concentration, and reduced the energy cost of the synthesis process. The material of the electrode significantly influenced the NH_3 production. Among the tested materials, including NiFe, SS, Ti, and Cu, the Cu electrode achieved the highest concentration of NH_3 (2983 ppm) and the lowest energy cost (90.2 MJ $mol_{NH_3}^{-1}$) at an N_2/H_2 molar ratio of 1:1 and a flow rate of 100 ml min^{-1}. This finding can be attributed to the chemisorption properties of the tangled electrode. By changing the total flow rate and the N_2/H_2 molar ratio in the feed gas, the production of NH_3 can be further optimised. The energy cost for the NH_3 synthesis dropped to 59.0 MJ $mol_{NH_3}^{-1}$ when using the Cu electrode at a flow rate of 250 ml min^{-1}. In addition, the effect of electrode material on the electrical properties of the reactor was discussed. Compared to the DBD using the rod electrode, the use of tangled wire electrodes decreased the breakdown voltage and enhanced charge deposition, both of which contributed to the

enhanced NH_3 production. The possible reaction pathways for the plasma NH_3 synthesis were discussed with a view to providing knowledge for the future development of this attractive and emerging technology.

Acknowledgement

The support of this work by the UK EPSRC Impact Acceleration Account (IAA) is gratefully acknowledged. Y. Ma also acknowledges the PhD fellowship co-funded by the University of Liverpool and the Chinese Scholarship Council (CSC).

References

[1] FAO, World fertilizer trends and outlook to 2022, in, Rome, 2019.
[2] J.W. Erisman, M.A. Sutton, J. Galloway, Z. Klimont, W. Winiwarter, How a century of ammonia synthesis changed the world, Nature Geoscience, 1 (2008) 636-639.
[3] M. Kitano, Y. Inoue, Y. Yamazaki, F. Hayashi, S. Kanbara, S. Matsuishi, T. Yokoyama, S.-W. Kim, M. Hara, H. Hosono, Ammonia synthesis using a stable electride as an electron donor and reversible hydrogen store, Nature Chemistry, 4 (2012) 934-940.
[4] C. Smith, A.K. Hill, L. Torrente-Murciano, Current and future role of Haber–Bosch ammonia in a carbon-free energy landscape, Energy & Environmental Science, 13 (2020) 331-344.
[5] L.R. Winter, B. Ashford, J. Hong, A.B. Murphy, J.G. Chen, Identifying Surface Reaction Intermediates in Plasma Catalytic Ammonia Synthesis, ACS Catalysis, 10 (2020) 14763-14774.
[6] D.E. Canfield, A.N. Glazer, P.G. Falkowski, The evolution and future of Earth's nitrogen cycle, Science, 330 (2010) 192-196.
[7] T. Kandemir, M.E. Schuster, A. Senyshyn, M. Behrens, R. Schlögl, The Haber-Bosch process revisited: On the real structure and stability of "ammonia Iron" under working conditions, Angewandte Chemie International Edition, 52 (2013) 471-477.
[8] J.G. Chen, R.M. Crooks, L.C. Seefeldt, K.L. Bren, R.M. Bullock, M.Y. Darensbourg, P.L. Holland, B. Hoffman, M.J. Janik, A.K. Jones, M.G. Kanatzidis, P. King, K.M. Lancaster, S.V. Lymar, P. Pfromm, W.F. Schneider, R.R. Schrock, Beyond fossil fuel–driven nitrogen transformations, Science, 360 (2018) eaar6611.
[9] L.R. Winter, J.G. Chen, N2 Fixation by Plasma-Activated Processes, Joule, 5 (2021) 300-315.
[10] A. Bogaerts, X. Tu, J.C. Whitehead, G. Centi, L. Lefferts, O. Guaitella, F. Azzolina-Jury, H.-H. Kim, A.B. Murphy, W.F. Schneider, T. Nozaki, J.C. Hicks, A. Rousseau, F. Thevenet, A. Khacef, M. Carreon, The 2020 plasma catalysis roadmap, Journal of Physics D: Applied Physics, 53 (2020) 443001.
[11] K. Liu, W. Ren, C. Ran, R. Zhou, W. Tang, R. Zhou, Z. Yang, K. Ostrikov, Long-lived species in plasma-activated water generated by an AC multi-needle-to-water discharge: effects of gas flow on chemical reactions, Journal of Physics D: Applied Physics, 54 (2020) 065201.
[12] P. Chawdhury, Y. Wang, D. Ray, S. Mathieu, N. Wang, J. Harding, F. Bin, X. Tu, C. Subrahmanyam, A promising plasma-catalytic approach towards single-step methane conversion to oxygenates at room temperature, Applied Catalysis B: Environmental, 284 (2021) 119735.
[13] L. Di, J. Zhang, X. Zhang, H. Wang, H. Li, Y. Li, D. Bu, Cold plasma treatment of catalytic materials: a review, Journal of Physics D: Applied Physics, 54 (2021) 333001.

[14] H. Chen, A. Wu, S. Mathieu, P. Gao, X. Li, B.Z. Xu, J. Yan, X. Tu, Highly efficient nitrogen fixation enabled by an atmospheric pressure rotating gliding arc, Plasma Processes and Polymers, 18 (2021) 2000200.
[15] L. Wang, Y. Yi, C. Wu, H. Guo, X. Tu, One-Step Reforming of CO2 and CH4 into High-Value Liquid Chemicals and Fuels at Room Temperature by Plasma-Driven Catalysis, Angewandte Chemie International Edition, 56 (2017) 13679-13683.
[16] A. Wu, J. Yang, B. Xu, X.-Y. Wu, Y. Wang, X. Lv, Y. Ma, A. Xu, J. Zheng, Q. Tan, Y. Peng, Z. Qi, H. Qi, J. Li, Y. Wang, J. Harding, X. Tu, A. Wang, J. Yan, X. Li, Direct ammonia synthesis from the air via gliding arc plasma integrated with single atom electrocatalysis, Applied Catalysis B: Environmental, (2021) 120667.
[17] X. Zhu, X. Hu, X. Wu, Y. Cai, H. Zhang, X. Tu, Ammonia synthesis over γ-Al2O3 pellets in a packed-bed dielectric barrier discharge reactor, Journal of Physics D: Applied Physics, 53 (2020) 164002.
[18] X. Hu, X. Zhu, X. Wu, Y. Cai, X. Tu, Plasma-enhanced NH3 synthesis over activated carbon-based catalysts: Effect of active metal phase, Plasma Processes and Polymers, 17 (2020) 2000072.
[19] J. Hong, M. Aramesh, O. Shimoni, D.H. Seo, S. Yick, A. Greig, C. Charles, S. Prawer, A.B. Murphy, Plasma catalytic synthesis of ammonia using functionalized-carbon coatings in an atmospheric-pressure non-equilibrium discharge, Plasma Chemistry and Plasma Processing, 36 (2016) 917-940.
[20] M. Bai, Z. Zhang, X. Bai, M. Bai, N. Wang, Plasma synthesis of ammonia with a microgap dielectric barrier discharge at ambient pressure, IEEE Transactions on Plasma Science, 31 (2003) 1285-1291.
[21] Y. Wang, M. Craven, X. Yu, J. Ding, P. Bryant, J. Huang, X. Tu, Plasma-Enhanced Catalytic Synthesis of Ammonia over a Ni/Al2O3 Catalyst at Near-Room Temperature: Insights into the Importance of the Catalyst Surface on the Reaction Mechanism, ACS Catalysis, 9 (2019) 10780-10793.
[22] K. Aihara, M. Akiyama, T. Deguchi, M. Tanaka, R. Hagiwara, M. Iwamoto, Remarkable catalysis of a wool-like copper electrode for NH_3 synthesis from N_2 and H_2 in non-thermal atmospheric plasma, Chem. Commun., 52 (2016) 13560-13563.
[23] M. Iwamoto, M. Akiyama, K. Aihara, T. Deguchi, Ammonia Synthesis on Wool-Like Au, Pt, Pd, Ag, or Cu Electrode Catalysts in Nonthermal Atmospheric-Pressure Plasma of N2 and H2, ACS Catalysis, 7 (2017) 6924-6929.
[24] P. Mehta, P. Barboun, F.A. Herrera, J. Kim, P. Rumbach, D.B. Go, J.C. Hicks, W.F. Schneider, Overcoming ammonia synthesis scaling relations with plasma-enabled catalysis, Nature Catalysis, 1 (2018) 269-275.
[25] H. Uyama, T. Nakamura, S. Tanaka, O. Matsumoto, Catalytic effect of iron wires on the syntheses of ammonia and hydrazine in a radio-frequency discharge, Plasma Chemistry and Plasma Processing, 13 (1993) 117-131.
[26] K.S. Yin, M. Venugopalan, Plasma chemical synthesis. I. Effect of electrode material on the synthesis of ammonia, Plasma Chemistry and Plasma Processing, 3 (1983) 343-350.
[27] U. Kogelschatz, Dielectric-Barrier Discharges: Their History, Discharge Physics, and Industrial Applications, Plasma Chemistry and Plasma Processing, 23 (2003) 1-46.
[28] K.P. Francke, R. Rudolph, H. Miessner, Design and Operating Characteristics of a Simple and Reliable DBD Reactor for Use with Atmospheric Air, Plasma Chemistry and Plasma Processing, 23 (2003) 47-57.
[29] X. Tu, H.J. Gallon, M.V. Twigg, P.A. Gorry, J.C. Whitehead, Dry reforming of methane over a Ni/Al2O3catalyst in a coaxial dielectric barrier discharge reactor, Journal of Physics D: Applied Physics, 44 (2011) 274007.
[30] H.E. Wagner, R. Brandenburg, K.V. Kozlov, A. Sonnenfeld, P. Michel, J.F. Behnke, The barrier discharge: basic properties and applications to surface treatment, Vacuum, 71 (2003) 417-436.

[31] L. Wang, Y.H. Yi, Y. Zhao, R. Zhang, J.L. Zhang, H.C. Guo, NH_3 decomposition for H_2 generation: Effects of cheap metals and supports on plasma–Catalyst synergy, ACS Catalysis, 5 (2015) 4167-4174.
[32] P. Peng, Y. Cheng, R. Hatzenbeller, M. Addy, N. Zhou, C. Schiappacasse, D. Chen, Y. Zhang, E. Anderson, Y. Liu, P. Chen, R. Ruan, Ru-based multifunctional mesoporous catalyst for low-pressure and non-thermal plasma synthesis of ammonia, International Journal of Hydrogen Energy, 42 (2017) 19056-19066.
[33] A. Gómez-Ramírez, J. Cotrino, R.M. Lambert, A.R. González-Elipe, Efficient synthesis of ammonia from N_2 and H_2 alone in a ferroelectric packed-bed DBD reactor, Plasma Sources Science and Technology, 24 (2015) 065011.
[34] J. Hong, S. Pancheshnyi, E. Tam, J.J. Lowke, S. Prawer, A.B. Murphy, Corrigendum: Kinetic modelling of NH3 production in N2–H2 non-equilibrium atmospheric-pressure plasma catalysis (2017 J. Phys. D: Appl. Phys. 50 154005), Journal of Physics D: Applied Physics, 51 (2018) 109501.
[35] H.-H. Kim, Y. Teramoto, A. Ogata, H. Takagi, T. Nanba, Atmospheric-pressure nonthermal plasma synthesis of ammonia over ruthenium catalysts, Plasma Processes and Polymers, 14 (2017) 1600157.
[36] P. Peng, Y. Li, Y. Cheng, S. Deng, P. Chen, R. Ruan, Atmospheric pressure ammonia synthesis using non-thermal plasma assisted catalysis, Plasma Chemistry and Plasma Processing, 36 (2016) 1201-1210.
[37] T. Mizushima, K. Matsumoto, H. Ohkita, N. Kakuta, Catalytic Effects of Metal-loaded Membrane-like Alumina Tubes on Ammonia Synthesis in Atmospheric Pressure Plasma by Dielectric Barrier Discharge, Plasma Chemistry and Plasma Processing, 27 (2007) 1-11.
[38] Y. Ma, J.D. Harding, X. Tu, Catalyst-free low temperature conversion of n-dodecane for co-generation of COx-free hydrogen and C2 hydrocarbons using a gliding arc plasma, International Journal of Hydrogen Energy, 44 (2019) 26158-26168.
[39] G. Ertl, Elementary Steps in Ammonia Synthesis, in: J.R. Jennings (Ed.) Catalytic Ammonia Synthesis: Fundamentals and Practice, Springer US, Boston, MA, 1991, pp. 109-132.
[40] P. Mehta, P. Barboun, D.B. Go, J.C. Hicks, W.F. Schneider, Catalysis Enabled by Plasma Activation of Strong Chemical Bonds: A Review, ACS Energy Letters, 4 (2019) 1115-1133.
[41] A. Gómez-Ramírez, A.M. Montoro-Damas, J. Cotrino, R.M. Lambert, A.R. González-Elipe, About the enhancement of chemical yield during the atmospheric plasma synthesis of ammonia in a ferroelectric packed bed reactor, Plasma Processes and Polymers, 14 (2017) 1600081.
[42] D. Zhou, R. Zhou, R. Zhou, B. Liu, T. Zhang, Y. Xian, P.J. Cullen, X. Lu, K. Ostrikov, Sustainable ammonia production by non-thermal plasmas: Status, mechanisms, and opportunities, Chemical Engineering Journal, 421 (2021) 129544.
[43] J. Hong, S. Prawer, A.B. Murphy, Plasma Catalysis as an Alternative Route for Ammonia Production: Status, Mechanisms, and Prospects for Progress, ACS Sustainable Chemistry & Engineering, 6 (2018) 15-31.
[44] J.R. Shah, J.M. Harrison, M.L. Carreon, Ammonia Plasma-Catalytic Synthesis Using Low Melting Point Alloys, Catalysts, 8 (2018) 437.
[45] J. Nakajima, H. Sekiguchi, Synthesis of ammonia using microwave discharge at atmospheric pressure, Thin Solid Films, 516 (2008) 4446-4451.
[46] J. Shah, W. Wang, A. Bogaerts, M.L. Carreon, Ammonia Synthesis by Radio Frequency Plasma Catalysis: Revealing the Underlying Mechanisms, ACS Applied Energy Materials, 1 (2018) 4824-4839.
[47] J. Shah, T. Wu, J. Lucero, M.A. Carreon, M.L. Carreon, Nonthermal Plasma Synthesis of Ammonia over Ni-MOF-74, ACS Sustainable Chemistry & Engineering, 7 (2019) 377-383.
[48] D. Xie, Y. Sun, T. Zhu, X. Fan, X. Hong, W. Yang, Ammonia synthesis and by-product formation from H2O, H2 and N2 by dielectric barrier discharge combined with an Ru/Al2O3 catalyst, RSC Advances, 6 (2016) 105338-105346.

[49] G. Akay, K. Zhang, Process Intensification in Ammonia Synthesis Using Novel Coassembled Supported Microporous Catalysts Promoted by Nonthermal Plasma, Industrial & Engineering Chemistry Research, 56 (2017) 457-468.
[50] T. Mizushima, K. Matsumoto, J.-i. Sugoh, H. Ohkita, N. Kakuta, Tubular membrane-like catalyst for reactor with dielectric-barrier-discharge plasma and its performance in ammonia synthesis, Applied Catalysis A: General, 265 (2004) 53-59.

Highlights

- Plasma synthesis of ammonia was carried out using a DBD plasma reactor.
- Using a tangled wire electrode enhanced the production of ammonia.
- The optimal energy efficiency for ammonia production was achieved using a Cu tangled electrode.

Declaration of interests

☒ The authors declare that they have no known competing financial interests or personal relationships that could have appeared to influence the work reported in this paper.

☐The authors declare the following financial interests/personal relationships which may be considered as potential competing interests: